Molecular Therapy
Oncology
Original Article

# Development of a novel, high-efficacy oncolytic herpes simplex virus type 1 platform equipped with two distinct retargeting modalities

Hyun-Yoo Joo,[1] Hyunjung Baek,[1] Chun-Seob Ahn,[1] Eun-Ran Park,[1] Youngju Lee,[1] Sujung Lee,[1] Mihee Han,[1] Bora Kim,[1] Yong-Hoon Jang,[1] and Heechung Kwon[1,2]

[1]Gencellmed Inc., Korea Institute of Radiological and Medical Sciences, Room 302 Research Building #3, Seoul, Republic of Korea; [2]Division of Radiation Biomedical Research, Korea Institute of Radiological and Medical Sciences, Seoul, Republic of Korea

**To retarget oncolytic herpes simplex virus (oHSV) to cancer-specific antigens, we designed a novel, double-retargeted oHSV platform that uses single-chain antibodies (scFvs) incorporated into both glycoprotein H and a bispecific adapter expressed from the viral genome to mediate infection predominantly via tumor-associated antigens. Successful retargeting was achieved using a nectin-1-detargeted HSV that remains capable of interacting with herpesvirus entry mediator (HVEM), the second canonical HSV entry receptor, and is, therefore, recognized by the adapter consisting of the virus-binding N-terminal 82 residues of HVEM fused to the target-specific scFv. We tested both an epithelial cell adhesion molecule (EpCAM)- and a human epidermal growth factor receptor 2-specific scFv separately and together to target cells expressing one, the other, or both receptors. Our results show not only dose-dependent, target receptor-specific infection *in vitro*, but also enhanced virus spread compared with single-retargeted virus. In addition, we observed effective infection and spreading of the EpCAM double-retargeted virus *in vivo*. Remarkably, a single intravenous dose of the EpCAM-specific virus eliminated all detectable tumors in a subcutaneous xenograft model, and the same intravenous dose seemed to be harmless in immunocompetent FVB/N mice. Our findings suggest that our double-retargeted oHSV platform can provide a potent, versatile, and systemically deliverable class of anti-cancer therapeutics that specifically target cancer cells while ensuring safety.**

## INTRODUCTION

In recent years, oncolytic viruses (OVs) have become a highly attractive treatment in cancer immunotherapy.[1–3] Antitumor effects of OVs are exerted through two mechanisms of action: (i) OVs specifically infect and replicate in tumor cells, eventually killing them, and (ii) the infection stimulates the host's innate and adaptive immunity against tumors. Among the OVs, herpes simplex virus (HSV) is the most widely studied for the treatment of solid tumors and accounts for nearly a quarter of all ongoing clinical trials. Amgen's herpesvirus Talimogene laherparepvec is the first and only U.S. Food and Drug Administration-approved OV for the treatment of metastatic melanoma.[4,5] Most recently, G47Δ (teserpaturev), a triple-mutated recombinant oncolytic HSV (oHSV), has been approved for the treatment of malignant glioma in Japan.[6] The tumor specificity of oHSV is typically a consequence of attenuating mutations in the viral genome that support a high safety profile by preventing replication in normal cells. These attenuated viruses exert activity against various tumors, but a potential drawback is that they replicate less efficiently in cancers than wild-type (WT) viruses, producing less oncolytic progeny.[7] Systemic administration of OVs remains of limited utility due to low efficiency of targeted delivery.

Strategies have been developed to redirect the natural viral tropism to tumor-specific antigens of choice without impairing the lytic potential of the virus. The main strategy developed for oHSV retargeting to cancers has involved the insertion of a peptide ligand, receptor ligand or single-chain antibody (scFv) into a viral attachment and/or entry glycoprotein. For example, successful targeting has been achieved by incorporation of ligands or scFv recognizing the human epidermal growth factor (EGF) receptor 2 (HER2),[8] the interleukin-13 receptor IL-13R,[9] the urokinase plasminogen activator receptor,[10] EGF receptor-vIII (EGFR-vIII),[11] or EGFR[12] into one or more of glycoprotein D (gD), glycoprotein C (gC), glycoprotein B (gB), and glycoprotein H (gH). An alternative retargeting strategy involves the use of soluble adapter molecules that are capable of binding to both HSV and a specific receptor on the surface of a target cell.[13,14] In a previous study, we reported that HSV could be specifically targeted to gastric carcinoma cells by an adapter protein composed of the N-terminal 82 residues of the normal, but narrowly distributed HSV receptor herpesvirus entry mediator (HVEM), fused to an anti-carcinoembryonic antigen (CEA) scFv.[13] CEA-specific virus entry was accomplished by combining the bispecific adapter with an HVEM-restricted gD-mutant virus that does not recognize the widely expressed HSV receptor nectin-1.[15]

Received 13 July 2023; accepted 16 February 2024;
https://doi.org/10.1016/j.omton.2024.200778.

**Correspondence:** Heechung Kwon, Gencellmed Inc., Room 302 Research Building #3, Korea Institute of Radiological and Medical Sciences, 75 Nowon-ro, Nowon-gu, Seoul 01812, Republic of Korea.
**E-mail:** hck1607@gencellmed.com

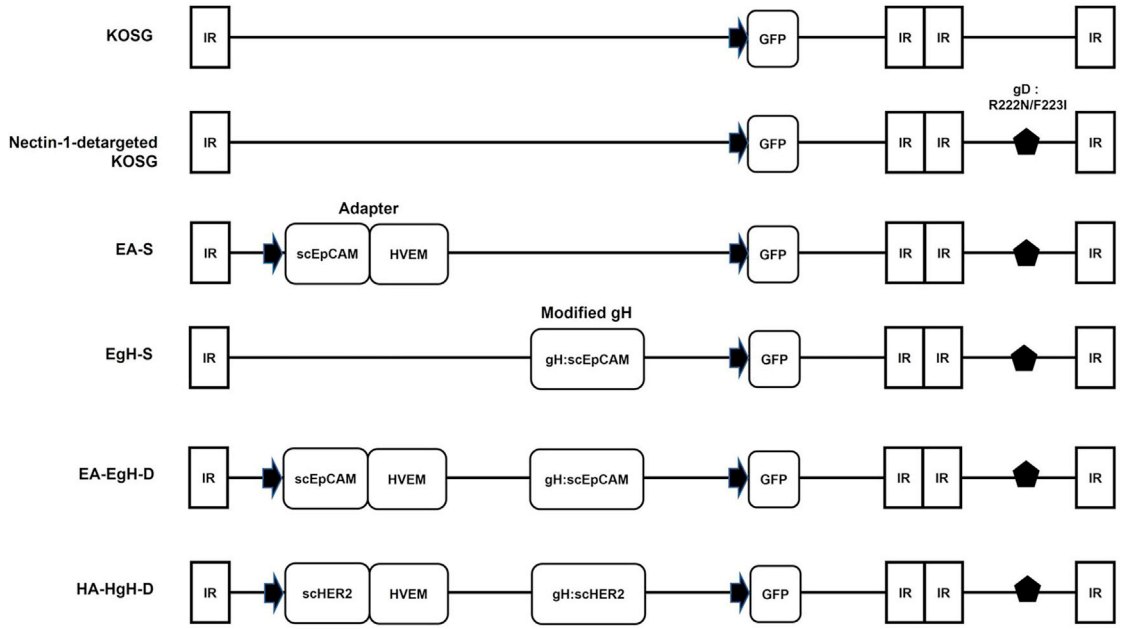


**Figure 1. Genome structures of the retargeted and control oncolytic herpesviruses used in this study**

Schematic representations of the genomes of KOSG (KOS-37 BAC-expressing GFP) and derivatives. All constructs except KOSG contained substitutions of Arg-222 and Phe-223 of gD to asparagine and isoleucine (R222N/F223I) for detargeting from the natural receptor nectin-1 (black diamond). Sequences encoding self-targeting adapters (scFvEpCAM-HVEM and scFvHER2-HVEM) and retargeted gH (gH:scFvEpCAM and gH:scFvHER2) were incorporated into the UL3/4 intergenic region and between codons 29 and 30 of the viral gH gene, respectively. Transgenes were transcribed from the CMV promoter (black arrow). D, (double) two retargeting genes in the HSV genome; S, single retargeted gene in the HSV genome.

Although the adapter-conjugated HSV showed reasonable efficiency of retargeted transduction both *in vitro* and *in vivo*, it required the continuous addition of the mixture of adapter protein and virus. The possibility that this limitation may be overcome by expression of the adapter from the viral genome has been validated in different replication-competent viral systems, including adenovirus and mouse hepatitis virus (MHV).[16–19] However, these single-component systems can suffer from genetic instability or otherwise low expression levels of the adapter.[20] In the present study, we successfully developed a novel self-targeting oHSV system for multi-round infection by expressing an EpCAM-HSV gD bridging adapter from an HVEM-restricted mutant HSV, providing sustained secretion of adapter molecules during viral replication in infected tumor cells. To enable initial retargeted infection without addition of exogenous adapter, we genetically targeted viral gH to the same or a different tumor-associated antigen, EpCAM or HER2. Our results with the doubly EpCAM-retargeted virus showed that both the initial infection and subsequent viral spread depend on cellular EpCAM expression in a dose-dependent manner. Our work highlights the potential of our double retargeting oHSV platform to serve as a highly specific and efficient delivery tool of oncolytic activity.

## RESULTS

### Generation of EpCAM-targeted oHSVs

In this study, we chose human EpCAM as the cancer-specific target receptor. EpCAM is a type I transmembrane glycoprotein overexpressed on the surface of various cancer cells.[21] As a strategy to construct a series of HSV recombinants simultaneously retargeted to EpCAM and detargeted from the natural receptor nectin-1, we genetically engineered KOS-37 bacterial artificial chromosome (BAC), a BAC carrying a complete HSV-1 strain KOS genome.[22] We inserted a GFP gene under the control of an immediate-early viral promoter in the UL26-UL27 intergenic region to produce KOSG BAC, and modified the gD gene of KOSG BAC to encode a nectin-1-detargeted mutant protein, $gD^{R222N/F223I}$.[15] We then constructed three derivatives of nectin-1-detargeted KOSG BAC (Figure 1): (i) EA-S, carrying an expression cassette in the UL3-UL4 intergenic region for an adapter, scFvEpCAM, composed of an anti-EpCAM scFv fused with the gD-binding N-terminal 82 residues of HVEM; (ii) EgH-S, carrying an insertion of the anti-EpCAM scFv open reading frame between codons 29 and 30 of the viral gH gene; and (iii) EA-EgH-D, carrying both the adapter expression cassette and the modified gH gene. In addition, we used an anti-HER2 scFv to generate HA-HgH-D, a HER2-specific counterpart of EA-EgH-D. Each recombinant was verified by pulse field gel electrophoresis analysis and DNA sequencing through the modified region(s). BAC constructs were transfected into Cre- and HVEM-expressing Vero cells (Cre-Vero-HVEM) to remove the loxP-bracketed BAC sequences, and recombinant viruses were propagated in Vero-HVEM cells. The expression of adapter and modified gH was confirmed by western blot analysis of supernatants from infected MDA-MB-453 cells with anti-His and anti-gH antibodies, showing that the adapter proteins

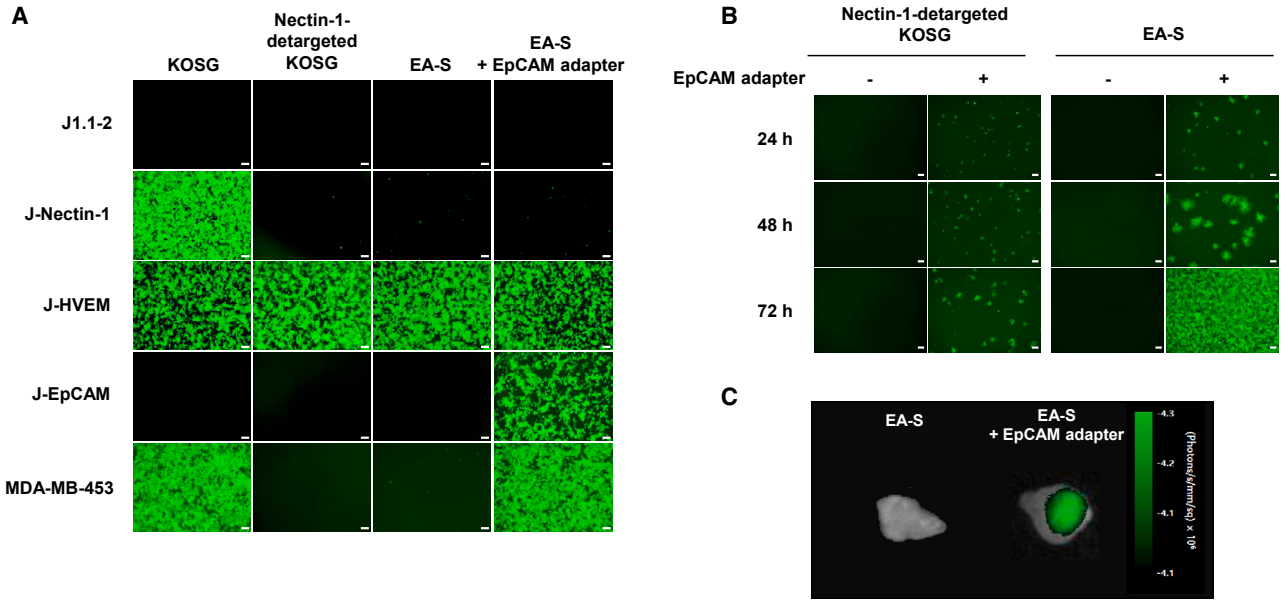


**Figure 2. Infection and spread of self-targeting adapter-expressing oHSV-1 (EA-S) in EpCAM-expressing cell lines**

(A) Infection of EpCAM-expressing cell lines by EA-S with or without adapter protein. J1.1-2, J-Nectin-1, J-HVEM, and J-EpCAM cells were infected at an MOI of 3 and MDA-MB-453 cells were infected at an MOI of 1. Scale bars, 100 μm. (B) Spreading of EA-S by self-targeting adapter expressed from the virus. MDA-MB-453 cells were infected with EA-S at an MOI of 0.01 in the presence or absence of EpCAM adapter, incubated at 37°C, and fluorescence recorded at 24, 48, and 72 h. Scale bars, 200 μm. (C) *In vivo* replication of EA-S treated with or without EpCAM adapter in MDA-MB-453 tumors. At 72 h after i.t. injection of EA-S with or without the EpCAM adapter, viral spreading was visualized by a GFP fluorescence *in vivo* imager.

were properly synthesized and secreted, and that the electrophoretic mobility of gH:scEpCAM was reduced compared with that of WT gH from KOSG (Figure S1).

### Initial infection and cell-to-cell spreading of EA-S virus in EpCAM-expressing cells

In our previous study, we showed that the nectin-1-detargeted $gD^{R222N/F223I}$ mutant virus K-222/3NI initially infected CEA-expressing gastric cancer cells in the presence of a CEA-$gD^{R222N/F223I}$ bridging adapter referred to here as scFvCEA-HVEM, but this strategy is limited by the necessity to combine purified adapter protein with the virus not only to initiate, but also subsequently to vigorously expand the retargeted infection.[13] To circumvent this limitation, we developed a self-targeting system by incorporating an expression cassette for the adapter into the viral genome, thereby allowing the virus to produce the adapter in infected cells. To determine whether this system is sufficient to mediate both entry and spread of the virus without exogenous supply of adapter protein, we infected various cell lines with EA-S virus in the presence or absence of recombinant scFvEpCAM-HVEM adapter (HA) protein (EpCAM adapter) and visualized the results by GFP imaging. The specificity of viral infection was determined using J1.1-2 cells, which do not express any gD receptors, their derivatives (J-Nectin-1, J-HVEM, and J-EpCAM), and EpCAM-expressing human MDA-MB-453 cells. As shown in Figure 2A, KOSG did not infect J1.1-2 and J-EpCAM cells, whereas the virus efficiently entered into J-nectin-1 and J-HVEM. Nectin-1-detargeted KOSG and EA-S virus, containing the substitutions in gD, infected J-HVEM cells as efficiently as KOSG, but failed to infect J-nectin-1- and nectin-1-positive MDA-MB-453 cells (Figure S2). EA-S also did not infect J-EpCAM cells, but when pre-treated with the scFvEpCAM-HA, was able to infect both MDA-MB-453 and J-EpCAM cells. These results indicated that the virus required an exogenous adapter for initial infection through the target receptor. However, once EA-S gained entry into MDA-MB-453 cells, it showed a remarkable ability to spread (Figure 2B), whereas no comparable spread was observed for nectin-1-detargeted KOSG under the same conditions, clearly demonstrating the ability of virus-expressed adapter to support expanding infection. Next, we explored the ability of EA-S to replicate in MDA-MB-453 tumors in nude mice. Subcutaneous (s.c.) MDA-MB-453 tumors were injected with EA-S in the presence or absence of the EpCAM adapter, and, upon resection 72 h later, the tumors were analyzed for virus-encoded GFP. As expected, EA-S-injected tumors did not show a GFP signal at 72 h. In contrast, evidence of robust replication was readily detectable in tumors inoculated with EA-S plus EpCAM adapter (Figure 2C). These results indicated that self-targeting EA-S can carry out a persistent, multi-round infection with efficient spread in cancer cells.

### Infection, spread, and specificity of EpCAM double-retargeted oHSV

To determine whether retargeting of gH to EpCAM would enable initial infection without a purified adapter, we infected J-derived cells

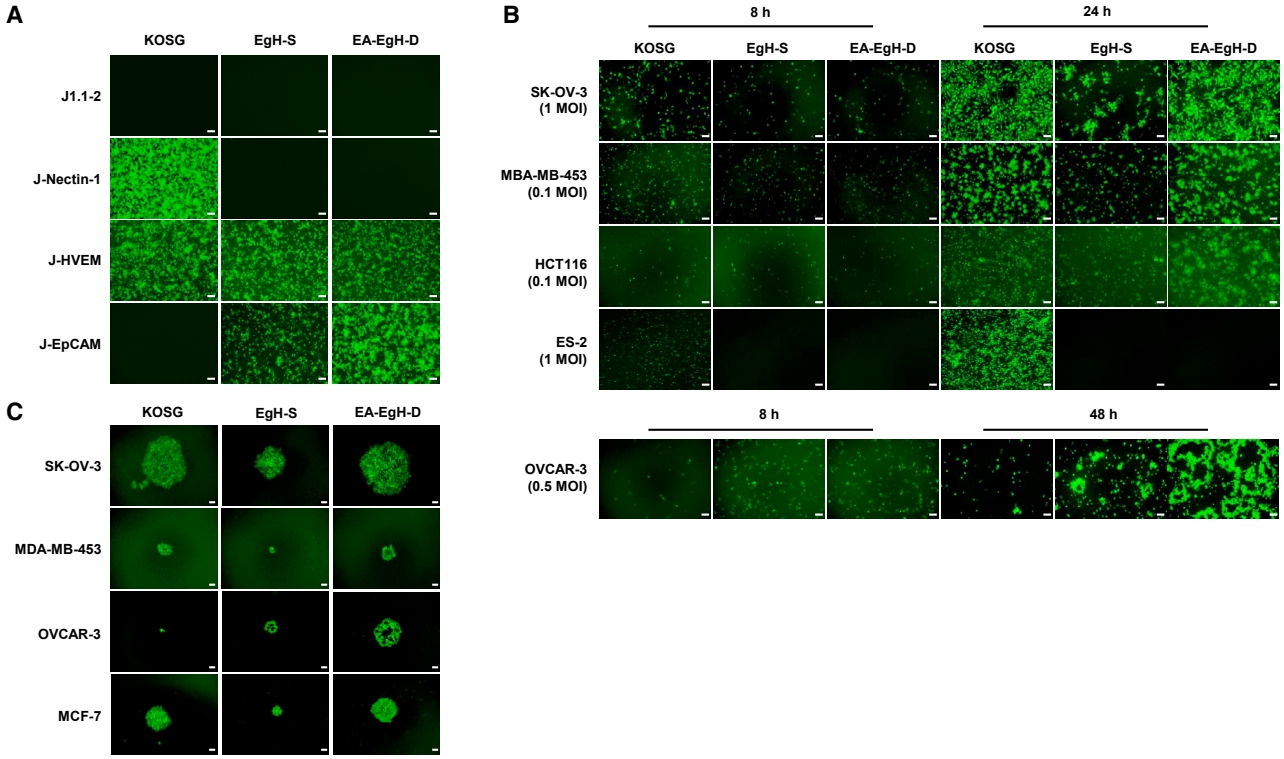


**Figure 3. Enhancement of viral entry and spread by double-retargeted oHSV-1 equipped with a self-targeting adapter and targeted gH**

(A) Entry specificity of double-retargeted oHSV-1. We used J-cell lines to examine the infection specificities of single and double-retargeted viruses, EgH-S and EA-EgH-D, respectively, at MOIs of 3 for 24 h. Scale bars, 200 μm. (B) Infection and spread of EA-EgH-D compared with KOSG and EgH-S in cancer cells. EpCAM-expressing cancer cell lines SK-OV-3 (1 MOI), MDA-MB-453 (0.1 MOI), OVCAR-3 (0.5 MOI), HCT116 (0.1 MOI), and EpCAM-negative ES-2 cells (1 MOI) were infected with KOSG or EpCAM-retargeted viruses and infection was recorded as green fluorescence at 8 and 24 or 48 h. Scale bars, 200 μm. (C) Plaques formed by KOSG, EgH-S, and EA-EgH-D on different cancer cell lines at 3 days after infection. Scale bars, 100 μm.

with KOSG, EgH-S, and EA-EgH-D at a multiplicity of infection (MOI) of 3. Figure 3A shows that the EgH-S and EA-EgH-D viruses, which both have the nectin-1-detargeting R222N/F223I substitutions in gD, failed to infect J-nectin-1 cells, but entered J-EpCAM cells, although not equally efficiently. The three viruses were further assayed for their abilities to enter EpCAM-positive (SK-OV-3, MDA-MB-453, HCT116, and OVCAR-3) and EpCAM-negative (ES-2) cancer cells; EpCAM, nectin-1, and HVEM levels on the surface of these cells were determined by fluorescence-activated cell sorting (FACS) (Figure S2). As shown in Figure 3B, EgH-S and EA-EgH-D were able to enter EpCAM-positive cancer cells, but failed to enter EpCAM-negative ES-2 cells. Additionally, while EgH-S and EA-EgH-D seemed to exhibit a similar entry rate in the early infection period (8 h after infection), EA-EgH-D infection seemed to have spread significantly more than infection by EgH-S at 24 h (SK-OV-3, MDA-MB-453, and HCT116 cells) and 48 h (OVCAR-3 cells). We further analyzed cell-to-cell spread by comparing plaque sizes between the viruses at 3 days after infection. As illustrated with the representative images of Figure 3C, EA-EgH-D and KOSG produced similarly sized plaques that were 2.1- and 2.5-fold larger than those formed by EgH-S on both SK-OV-3 and MCF-7 cells. In OVCAR-3 cells, KOSG showed low infection and spreading, likely due to the relatively low amount of nectin-1 on the surface of these cells (Figure S2), but here, too, EA-EgH-D showed greater spread than EgH-S. Taken together, these results indicated that the retargeted gH was sufficient to enable virus entry through EpCAM recognition and that virus-mediated expression of the adapter substantially enhanced lateral virus spread. To further confirm the receptor specificity of EA-EgH-D infection, we performed a blocking assay by pre-incubation of the cells with anti-EpCAM or control monoclonal antibody. As shown in Figure S3, EA-EgH-D entry and cell-to-cell spread in cancer cell lines were dramatically inhibited by pre-treatment of the cells with EpCAM-specific, but not isotype-matched, control antibody. In contrast, entry of KOSG was not affected by the anti-EpCAM antibody. We concluded that the entry of EA-EgH-D depends on EpCAM, since it was inhibited by EpCAM-specific antibody.

### Killing ability and replication of EA-EgH-D virus in cancer cell lines

To investigate the killing ability of EA-EgH-D virus, we infected several of the cancer cell lines characterized earlier for cell-surface

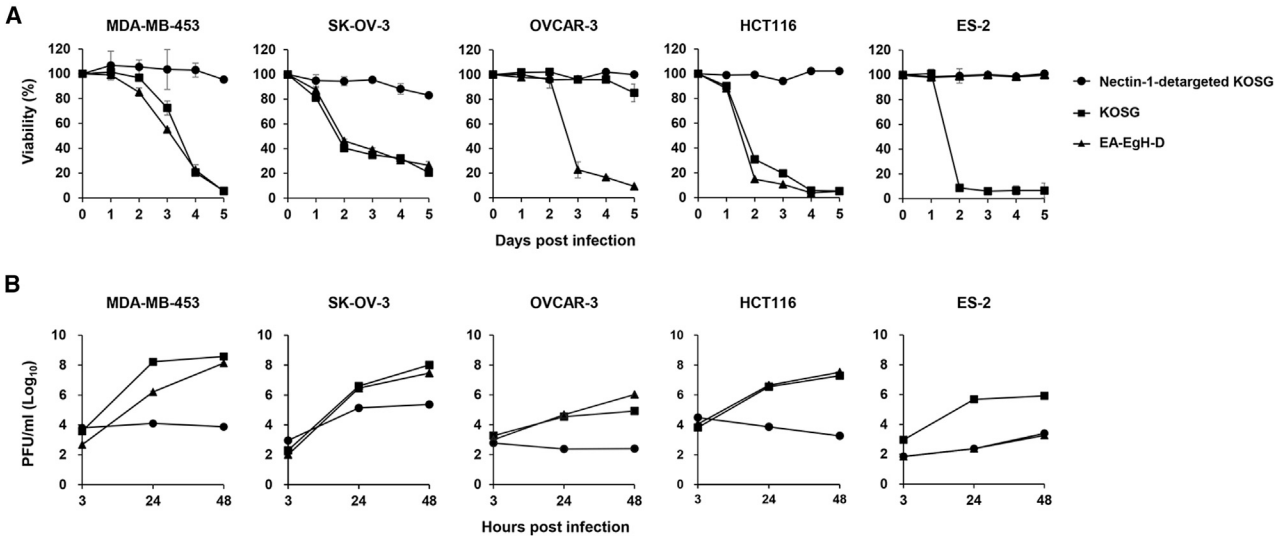


**Figure 4. Killing ability and replication of EA-EgH-D in EpCAM-expressing cancer cells**

(A) Cytotoxicity of EA-EgH-D for EpCAM-expressing cancer cell lines. Cancer cells were infected at an MOI of 1, and percent cell viability relative to uninfected cells was assessed by WST-1 assay daily for 5 days. Controls included EpCAM-negative ES-2 cells and infections with KOSG and nectin-1-detargeted KOSG. (B) Analysis of EA-EgH-D replication in comparison with that of KOSG and nectin-1-detargeted KOSG. Cancer cells were infected at an MOI of 0.1, the cells were harvested and lysed at the indicated times after infection, and progeny titers determined by plaque assay on Vero-HVEM cells. Controls were as in (A). All data are presented as the mean ± standard error of the mean.

EpCAM abundance (Figure S2) with KOSG or EA-EgH-D at an MOI of 1, and determined cell viability daily for 5 days by WST-1 assay. EA-EgH-D killed all five EpCAM-positive cell lines tested, while EpCAM-negative ES-2 cells were resistant (Figure 4A). The control virus, KOSG, killed all of the cell lines with the exception of OVCAR-3 cells, which display little or no nectin-1 on their surface (Figure S2). In contrast, nectin-1-detargeted KOSG did not show substantial cytotoxicity for any of the cell lines. The relative cell killing efficiencies of EA-EgH-D on the different cell lines correlated with the relative entry efficiencies of the virus into the same cell lines (Figure 3B), which in turn correlated with cell-surface EpCAM levels (Figure S2). Of note, the cytotoxicity of EA-EgH-D appeared similar to that of KOSG. We also compared the replication efficiencies of EA-EgH-D and KOSG in the same cancer cell lines. As shown in Figure 4B, the two viruses grew at similar rates in all of the EpCAM-positive cell lines, including relatively slow growth in OVCAR-3 cells, and the only major difference between the two viruses was seen in EpCAM-negative ES-2 cells. Furthermore, the 48-h yields of EA-EgH-D and KOSG from EpCAM-positive, nectin-1-positive cells were largely similar. Again consistent with the low nectin-1 level on OVCAR-3 cells, however, the yield of nectin-1-dependent KOSG on these cells was some 10-fold lower than that of EA-EgH-D. Together, these results were indicative of robust EA-EgH-D replication and cytotoxicity on par with that of KOSG in susceptible cells.

### *In vivo* antitumor activity of double-retargeted EA-EgH-D virus

We explored the ability of EA-EgH-D to replicate in established EpCAM-positive tumors in BALB/c nude mice. To visualize *in vivo* replication, nude mice bearing s.c. MDA-MB-453 tumors were injected intratumorally (i.t.) with EA-EgH-D, and virus-mediated GFP expression was analyzed in tumors resected at 6, 48, and 72 h after virus inoculation. GFP was barely detectable at 6 h, but robust fluorescence was recorded at 72 h (Figure 5A). To assess the *in vivo* antitumor activity of EA-EgH-D, MDA-MB-453 tumors were allowed to grow until they reached an average volume of 100–150 $mm^3$, and were then injected with 10-fold escalating virus doses from $2 \times 10^4$ to $2 \times 10^6$ plaque-forming unit (PFU). As illustrated in Figure 5B, PBS-injected tumors grew from a mean ± SEM of 125.8 ± 32.9 $mm^3$ to a mean of 409.5 ± 158.4 $mm^3$ over a period of 50 d from the time of treatment. In contrast, the sizes of tumors injected with $2 \times 10^6$ PFU of EA-EgH-D declined from 124.5 ± 29.7 $mm^3$ to a mean of 6.2 ± 13.7 $mm^3$, with 4 out of 5 mice no longer carrying a detectable tumor in the final days of the 50 d observation period. At the lower EA-EgH-D doses, tumor growth was significantly delayed compared with the PBS control group ($p < 0.0001$, t test). We also explored the ability of our doubly EpCAM-retargeted oHSV to reach a target tumor and exert its antitumor activity after systemic administration. We tested three different doses of EA-EgH-D, from $2 \times 10^6$ to $2 \times 10^8$ PFU, administered through the tail vein of MDA-MB-453 tumor-bearing mice. In the PBS control group, tumors grew to a mean of 423 ± 38.8 $mm^3$ over a period of 38 d, but in the group injected with the highest dose of EA-EgH-D virus, tumors were no longer detectable at the end of this period in any of the mice (Figure 5C).

### *In vivo* safety of nectin-detargeted EA-EgH-D virus

To assess the effects of EA-EgH-D administration on survival and toxicity due to antiviral immune responses, we injected WT KOS (positive control) and EA-EgH-D into immunocompetent FVB/N

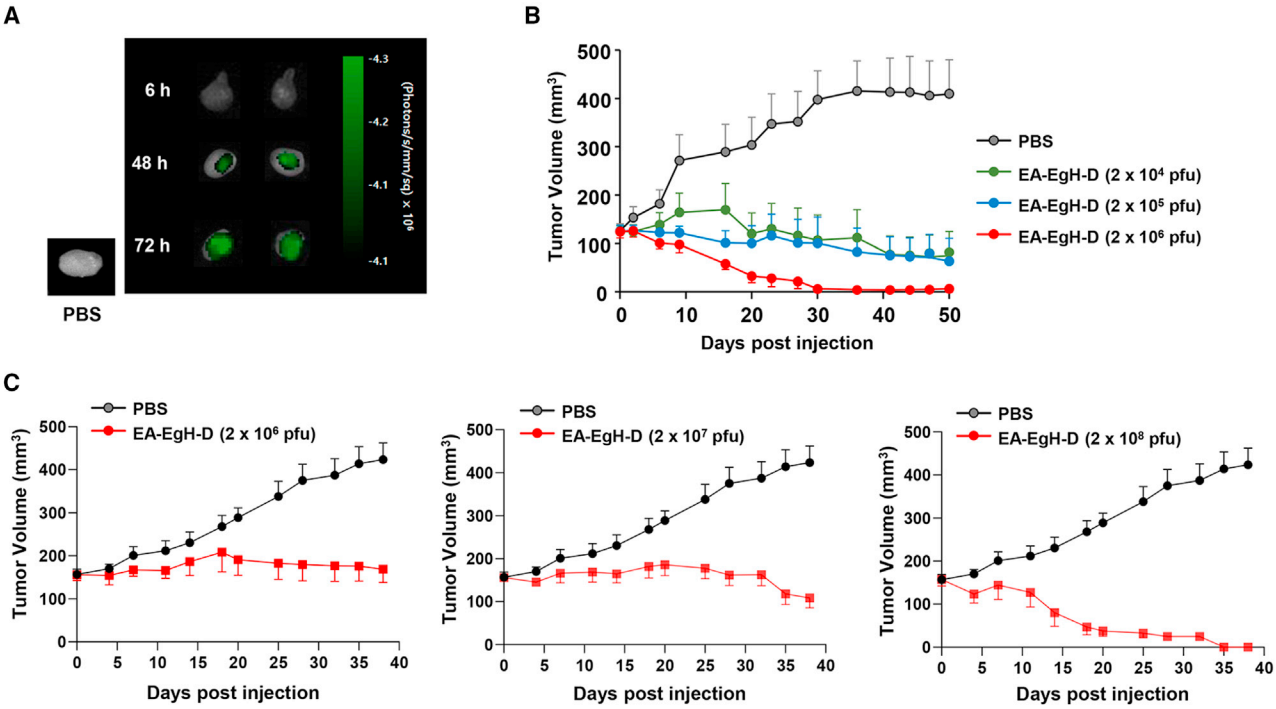


**Figure 5. Anti-tumor efficacy of double-retargeted oHSV-1 upon i.t. or i.v. administration in MDA-MB-453 xenograft model**

(A) *In vivo* replication and spread of EA-EgH-D. We injected $5 \times 10^6$ MDA-MB-453 cells s.c. into BALB/c nude mice. When the tumor volume reached approximately 130 $mm^3$, $2 \times 10^7$ PFU of EA-EgH-D was injected into the tumor mass. Viral replication in the tumor mass was observed under a fluorescence *in vivo* imager. (B) Dose-related anti-tumor efficacy of EA-EgH-D after i.t. administration. When the tumor volume reached approximately 130 $mm^3$, $2 \times 10^4$, $2 \times 10^5$, or $2 \times 10^6$ PFU of double-retargeted EA-EgH-D virus were injected directly into the MDA-MB-453 tumor mass. (C) Antitumor efficacy by systemic administration of EA-EgH-D at the indicated doses. Tumor-bearing mice (~200 $mm^3$) were i.v. administered $2 \times 10^6$, $2 \times 10^7$, or $2 \times 10^8$ PFU of virus via the tail vein. Tumor volumes were measured twice a week for 38 days and expressed as means ± standard error of the mean.

mice. We administered intravenous (i.v.) injections of $1 \times 10^6$ PFU KOS and $1 \times 10^8$ PFU EA-EgH-D virus into FVB/N mice and monitored their survival rates. After receiving a dose of $1 \times 10^6$ PFU KOS, all mice were observed to have an abnormal gait with apparent hindlimb paralysis, indicating that FVB/N mice are susceptible to human HSV-1 infection. In contrast, all mice injected with a single i.v. injection of $1 \times 10^8$ PFU EA-EgH-D survived more than 88 days, and no adverse events were observed (Figure 6A).

To assess the tissue distribution of the KOS and EA-EgH-D virus infections, genomic DNA was isolated from various organ tissues of mice 8 days after i.v. virus administration. This was done to confirm the distribution of the virus in the tissues. qPCR targeting the HSV-1 gD gene was conducted on various tissues and generated a standard curve ($10^2$–$10^8$) using 10-fold dilutions of known concentrations of HSV virus DNA. As depicted in Figure 6B, the number of KOS genome copies per 50 ng tissue DNA was notably higher in brain tissue compared with other tissues of the mice. Similarly, the genomic copies of EA-EgH-D, per 50 ng tissue DNA, were found to be lower across all examined tissues. These findings reveal that the mice injected with 100 times higher PFU of EA-EgH-D exhibited 20 times lower levels of HSV-1 copies in the brain tissue compared with those injected with KOS. This significant decrease indicates the relative safety of nectin-detargeted EA-EgH-D, particularly in terms of neurotoxicity, as opposed to KOS, and highlights the absence of adverse effects associated with HSV-1 in the EA-EgH-D group.

### Extension of the double retargeting oHSV platform to HER2-expressing cells

To expand the target range of our effective oHSV retargeting platform, we engineered HA-HgH-D containing anti-HER2 scFvs in both the virus-encoded targeting adapter and gH (Figure 1). Figure S4A illustrates that MDA-MB-453 and SK-OV-3 cells express HER2 on their surface while ES-2 cells do not. Exposure of these cells to HA-HgH-D at an MOI of 2 demonstrated widespread infection comparable to that by KOSG of the two HER2-positive cell lines at 24 h, but no infection of ES-2 cells (Figure S4B). In agreement with these results, the HER2 double-retargeted virus exhibited cytotoxic activity in HER2-positive MDA-MB-453 and SK-OV-3 but not in HER2-negative ES-2 cells, whereas KOSG displayed cytotoxicity for all three cell lines (Figure S4C). The successful generation of a viable HER2 doubly retargeted virus supports the possibility that our double retargeting oHSV platform can be applied to cancers that express different antigens.

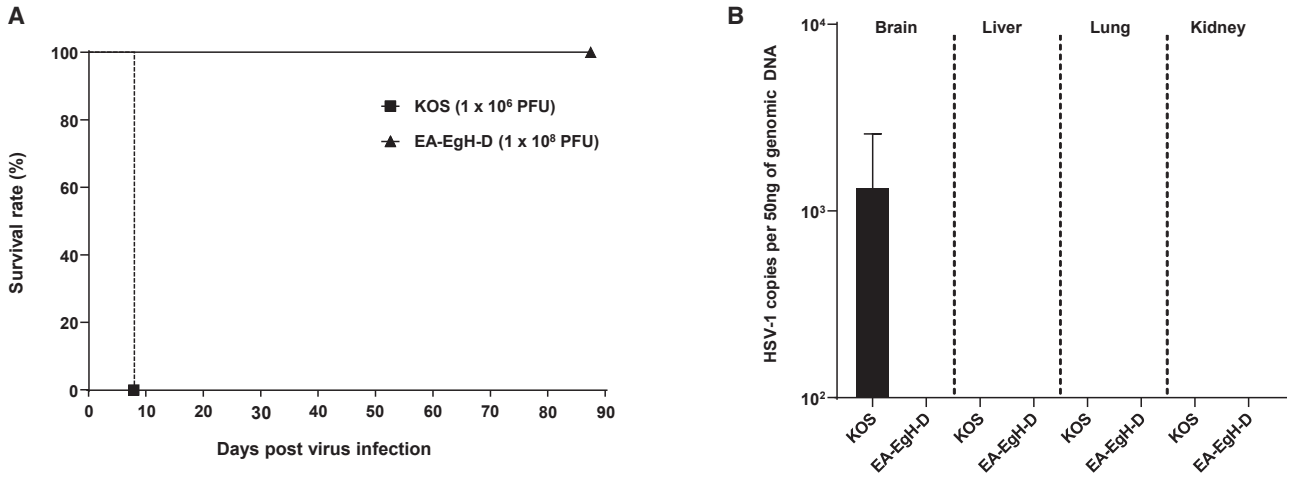


**Figure 6. *In vivo* safety assessment and biodistribution of double-targeting EA-EgH-D in FVB/N mice**

(A) Mice were injected i.v. with $1 \times 10^6$ PFU of KOS (n = 5) and $1 \times 10^8$ PFU of EA-EgH-D (n = 5). The survival rate was recorded by the Kaplan-Meier survival curve with observation for 88 days. (B) Distribution of HSV-1 in organs after i.v. injection with $1 \times 10^6$ PFU of KOS (n = 3) and $1 \times 10^8$ PFU of EA-EgH-D (n = 3). Organs were harvested on day 8, homogenized, and total DNA was extracted. Virus genome copy numbers were determined by qPCR compared with an expressed as genomic copies per 50 ng DNA. Each bars indicate the average and SD of the positive samples for each group.

## DISCUSSION

Various bispecific adapters have been developed for the targeted delivery of adenovirus, herpesvirus, and coronavirus vectors, including combinations with partially or completely detargeted viruses.[14,23,24] Several groups have reported that adapters consisting of target-specific scFvs fused to the soluble ectodomain of the coxsackie- and adenovirus receptor (sCAR) were able to retarget adenoviral vectors efficiently to cells expressing the scFv target, such as HER2, EGFR, and polysialic acid.[25–28] For multi-round transductional targeting, one group constructed a single-component OV, D24sCAR-EGF, by inserting an adapter expression cassette into a replication-competent adenoviral genome.[16] However, the oncolytic potency of this virus was severely impaired, suggesting that the expression of biologically active proteins can undermine virus replication.[17,29] Another group reported the generation of a self-targeting coronavirus, MHVsoR-EGF, which incorporated the coding sequence for an EGFR-targeting bispecific-adapter in the genome of MHV.[18] This virus showed EGFR-specific spread and cell killing in U87ΔEGFR cell cultures. However, the expression of scFv-containing adapter proteins from the MHV genome caused a detrimental degree of virus instability during propagation.[20] Bispecific adapters have also been developed for HSV retargeting to novel receptors. These strategies took into account the notion that soluble forms of the HSV receptors nectin-1 and HVEM can enable virus entry into receptor-deficient cells while inhibiting entry into receptor-bearing cells.[30,31] Bispecific adapters were developed that consisted of the gD-binding domain of nectin-1 or HVEM fused with an scFv directed against a tumor surface antigen, such as EGFR or CEA, enabling efficient HSV entry via the targeted receptor.[13,14] Although we and others have shown a reasonable efficiency *in vitro* and *in vivo* of retargeted cell transduction upon virus pre-incubation with adapter, these two-component systems allow only a single round of infection. Accordingly, it has been suggested that exogenously supplied adapters might be suitable for target-cell-specific transgene delivery by non-replicating but not replicating viral vectors.[32] While various adapters have been developed for virus retargeting to cancer cells, we report here the successful generation of recombinant viruses containing viral genome-encoded adapters consisting of a portion of a viral receptor and an scFv to a non-viral receptor. The virus-encoded EpCAM adapter is secreted after entry of EA-S virus into EpCAM-expressing cancer cells (Figure S1), which may be required for multi-round infection and lateral spread of virus to target cells *in vitro* and *in vivo*. Our results indicate that the strategy of expressing a retargeting adapter from the viral genome is effective in enhancing retargeted virus spread. Furthermore, the strategy can be readily modified to target more than one cancer-associated antigen with a single virus. However, spread by virus-encoded adapter still requires external adapter to initiate infection.

As noted previously, the HVEM-restricted gD-mutant virus requires further development to stabilize its receptor-restricted phenotype against reverting mutations, particularly for applications requiring replication.[13] The Campadelli-Fiume lab has reported a novel oHSV retargeting strategy involving the insertion of an scFv against HER2 into gH, either in a virus that retained the ability to enter via the canonical gD receptors or one lacking this ability.[8,33] They suggested that the modified gH with receptor-binding function could circumvent the requirement for gD-receptor interactions. This finding opened up a range of possibilities in HSV targeting, allowing modification of not only gD, but also gH as complete retargeting strategies. In this regard, we created the double-retargeted oHSV, EA-EgH-D, to establish a novel, high-efficiency strategy combining the self-targeting adapter and retargeted gH. The Campadelli-Fiume group described a double-retargeted HSV strategy to grow an

oHSV, fully detargeted from the natural HSV receptors and retargeted to, and, therefore, strictly dependent on, a cancer receptor, in a non-cancer cell line.[34] They engineered the 20-aa-long GCN4 peptide into the gH of their virus, which also carried the scFv to HER2 in gD. The production cell line was derived from Vero cells by expressing an artificial receptor capable of interacting with the GCN4 peptide in gH. Our own double-retargeted oHSV platform is different in that both of its targeting ligands are specific for cancer-associated receptors. Although the initial infection is mediated by only the scFv-fused gH, subsequent rounds of infection and spread seemed to be supported by both the modified gH and the endogenously supplied adapter, as evidenced by the larger plaques of the double EpCAM-retargeted virus than of the corresponding single retargeted viruses on the human cancer cells tested, resulting in similar effects as KOSG.

OVs have been developed for cancer patients, and more than 400 clinical trials have been conducted.[35] At present, i.t. delivery is the most common administration route for OV, while i.v. injection is approximately one-third as common. In contrast, i.t. injection of OVs can directly deliver higher numbers of viral particles into the target lesion than i.v. administration and generally with a high degree of safety. However, in clinical settings, i.t. infusion cannot be applied to patients with inaccessible or metastatic tumors. Therefore, systemic administration has been a key goal for the research and development of OVs, especially oHSVs. Systemic delivery requires that the virus effectively reaches and infects tumor lesions with sufficient potency to exert anticancer effects, while sparing non-tumor tissues to accomplish a high safety profile. We report here that tumor growth inhibition by a single i.v. injection of EA-EgH-D occurred in a dose-dependent manner, with complete regression of all tumors achieved in the highest dosage group. This double-retargeted oHSV, therefore, seems to hold promise as a systemically applicable antitumor agent. We also generated the HER2 doubly retargeted HA-HgH-D virus and showed its activity and specificity in cell culture, indicating that our platform for specific retargeting to cancer-specific receptors will be applicable to cancers expressing other antigens. In addition, these results show that our double-retargeted system could be switched into dual or triple-retargeted platforms for the treatment of heterogeneous tumors.

Since the activity of the adapter in our designs depends on preservation of the HVEM-binding surface of gD, the virus has the ability to interact with HVEM expressed on normal cells mainly in the spleen, thymus, bone marrow, lung and intestines that include T, B, and lymphoid cells.[36] Studies have shown that Nectin-1 knockout (KO) adult mice can be infected with HSV-1 through HVEM. Notably, HSV-1(F) infections in Nectin-1 KO adult mice did not show toxicity compared with normal mice.[37] For the OV rRP-450, which is based on HSV-1 and currently in phase I clinical trials, immunocompetent FVB/N mice were utilized to assess safety and distribution.[38] Consequently, we determined that the nectin-1-detargeted variant, EA-EgH-D, is safe for i.v. injection in FVB/N mice. Our toxicity data using WT KOS suggest it a suitable model. Uniformly, i.v. WT KOS virus was fatal at $10^6$ PFU and exhibited an abnormal gait with apparent hindlimb paralysis. By contrast, the IV administration of nectin-1-detargeted EA-EgH-D produced no adverse signs and symptoms in our studies. This phenomenon can be attributed to the distribution, where at least a 2,000-fold higher HSV-1 genome was detected in the brain tissue of KOS-injected mice compared with that of EA-EgH-D-injected mice. When examining the distribution of the virus in various tissues (brain, lung, liver, and kidney), viral DNA was rarely detected by qPCR. These findings imply that the nectin-1-detargeted EA-EgH-D is significantly less virulent than the WT virus, attenuated by at least 2,000-fold *in vivo*. Our results are consistent with the safety outcomes observed for the rRp450 virus in FVB/N mice, although in our study, the onset of lethality in the WT KOS-treated group was delayed by 5–6 days compared with the control group described by Currier et al.[38] Furthermore, our findings suggest that the nectin-1-detargeted EA-EgH-D is significantly less virulent than the WT virus, aligning with reports that Nectin-1 KO adult mice can be infected with HSV-1 through HVEM without observed toxicity compared with normal mice. However, additional research, particularly regarding the lethal dose via intracerebral administration, is necessary.

In addition, few if any tumor-associated receptors are unique to tumor cells and infection of normal cells expressing the same receptor, albeit typically at lower levels, is, therefore, not excluded, potentially causing off-tumor toxicity as described for chimeric antigen receptor (CAR)-T cells.[39] When considering the administration of the EA-EgH-D virus in humans, there remains uncertainty regarding its safety, particularly in relation to the infection of human tissues via HVEM. However, we will have a plan to devise sufficient alternative measures to ensure safety. As an alternative, it should be prudent to add additional features to the retargeted viruses that combine our transductional retargeting approach with transcriptional control of an essential viral gene, ICP6, by a tumor-specific promoter, human telomerase reverse transcriptase promoter, to minimize off-tumor effects and further improve safety.[40] Also for future clinical trials, we are preparing the removal of both LAT and UL56 genes from the EA-EgH-D virus to potentially decrease toxicity and inhibit virus reactivation in HVEM-expressing neurons.[41,42]

As further enhancements, our double-retargeted oHSV platform may be armed with cytokine genes promoting systemic antitumor immunity, and with the PH20 gene to provide hyaluronidase activity capable of degrading hyaluronan in the tumor extracellular matrix that limits the spread of OVs in tumor tissues.[43] In addition, to overcome the tumor heterogeneity of antigen expression and remove the immunosuppressive stromal cells expressing fibroblast-activation protein (FAP) that reside in the tumor microenvironment (TME), both of which were found as significant hurdles in CAR-T therapy,[44] another feasible approach may be triple-retargeted oHSVs containing, for example, a mesothelin-retargeted gH and expressing two adapters targeting different tumor-associated antigens, e.g., EpCAM and FAP.

Finally, our findings reveal the potential of our double EpCAM-retargeted oHSV to function as an effective, systemically deliverable

anti-cancer therapeutic, raising the expectation that this type of retargeted oHSV may well be suitable for the treatment of various types of cancers by different routes, including i.t., i.p., and i.v. Furthermore, we suggest that our double-retargeted oHSV platform expressing a self-targeting adapter and retargeted gH represents an attractive framework for the further development of novel strategies to target heterogeneous cancers and overcome the immunosuppressive TME.

## MATERIALS AND METHODS

### Cells and virus

African green monkey kidney cell line Vero (VERO01WCB-1201) was obtained from the Ministry of Food and Drug Safety. The following cell lines were obtained from the American Type Culture Collection: MDA-MB-453 (human breast carcinoma, HTB-131), MCF-7 (human breast adenocarcinoma, HTB-22), HCT116 (human colorectal carcinoma, CCL-247), SK-OV-3 (human ovarian serous cystadenocarcinoma, HTB-77), OVCAR-3 (human ovarian serous adenocarcinoma, HTB-161), and ES-2 (human ovarian clear adenocarcinoma, CRL-1978). Vero-HVEM and Cre-Vero-HVEM cells were established by transduction of Vero and Cre-Vero cells[22] with lentivirus expressing full-length human HVEM that was produced by transfection of 293FT cells with pLenti6-HVEM and selected for resistance to 10 μg/mL blasticidin (InvivoGen). Baby hamster kidney (J1.1-2) cell line and their derivatives expressing HVEM and nectin-1 were generous gift from Gabriella Campadelli-Fiume (University of Bologna). J-EpCAM cells were constructed by transduction of J1.1-2 cells with lentivirus containing human EpCAM and selected for resistance to 10 μg/mL blasticidin. SK-OV-3 cells were cultured in McCoy's 5A medium (Welgene) supplemented with 10% heat-inactivated fetal bovine serum (FBS, Welgene), 100 U/mL penicillin and 100 μg/mL streptomycin (Gibco). OVCAR-3 cells were cultured in Roswell Park Memorial Institute medium (RPMI-1640, Welgene) supplemented with 20% FBS, 10 μg/mL insulin (Sigma), 100 U/mL penicillin, and 100 μg/mL streptomycin. HepG2 and MDA-MB-453 cells were cultured in RPMI-1640 medium supplemented with 10% FBS, 100 U/mL penicillin, and 100 μg/mL streptomycin. MCF-7, J1.1-2, J-HVEM, and J-nectin1 cells were cultured in DMEM (Welgene) supplemented with 10% FBS, 100 U/mL penicillin and 100 μg/mL streptomycin. Vero-HVEM, Cre-Vero-HVEM, and J-EpCAM cells were grown in DMEM media supplemented with 10% FBS, 100 U/mL penicillin, 100 μg/mL streptomycin, and 5 μg/mL blasticidin for transgene expression. WT KOS strain was kindly provided by Joseph C. Glorioso (University of Pittsburgh) and was propagated and titrated on Vero cells.[45]

### Cloning of adapter and gH

A single-chain fragment variable of EpCAM (scFvEpCAM) was amplified from the synthetic vector pBHA-scEpCAM (4D5MOCB) by PCR with specific primers: forward 5′-GGGAAGCTTGCCACCATGAGTGTGCCCAC-3′ and reverse 5′-CCCGAATTCTGAACCGCCACCACCCGAGGAAACGGTCAGCAGCG-3′ with underlined restriction enzyme sites, *Hind*III and *Eco*RI. PCR was performed as follows: first denaturation at 95°C for 5 min, 30 cycles of amplification (95°C for 1 min, 60°C for 45 s, and 72°C 2 min), and final extension at 72°C for 5 min. To generate scFvEpCAM-HA, the pcDNA3.1-scFvCEA-HVEM vector[13] was digested with *Hind*III and *Eco*RI to remove scFvCEA region, and ligated with *Hind*III/*Eco*RI-digested scFvEpCAM gene. The ligated genes were transformed to *E. coli* (DH5α) and selected using antibiotics (ampicillin, 50 μg/mL). Recombinant adapter proteins were produced as previously described.[13]

To modify gH, scFvEpCAM gene was amplified using specific primers with *Not*I restriction enzyme site and linker sequences (forward, 5′-GCTGCGGCCGCCAGTAGTGGCGGTGGCTCTGGTTCCGGTGATATCCAGATGACCCAGTCC-3′; reverse, GCTGCGGCCGCGGATCCACCGGA ACCAGAGCCTCCACCGGAAGACGAGGAAACGGTCAGCAGCG). PCR was performed as follows: 1 cycle at 95°C for 5 min, 35 cycles at 95°C for 1 min, at 60°C for 45 s, and at 72°C for 2 min, and additional extension at 72°C for 5 min. The pPEP100-gH vector[46] was modified with *Not*I enzyme site between the 20 and 30 amino acid position (pPEP-gH29N). pEP-gH29N and scEpCAM were digested by *Not*I, ligated, and transformed into DH5α.

To engineer the adapter expression cassette, a scFv of HER2 (scFvHER2) was amplified from the sequence encoding the trastuzumab scFv by PCR with specific primers: forward 5′-CCCGGATCCGCCACCATGAGTGTGCCCACTCAGGTCCTGGGGTTGCTGCTGCTGTGGCTTACAGGTGCCAGATGTGAGGTGCAGCTGGTTG -3′ and reverse 5′- CCCGAATTCTGAACCGCCACCACCCTTGATTTCCACCTTGG -3′ with underlined restriction enzyme sites, *BamH*I and *Eco*RI. PCR amplification consisted of 1 cycle of 95°C for 5 min, followed by 30 cycles of 95°C for 1 min, 60°C for 45 s, 72°C for 2 min, and a final extension at 72°C for 5 min. To generate an scFvHER2-HA, the pcDNA3.1-scFvCEA-HVEM vector was digested with *BamH*I and *Eco*RI to remove the scFvHER2 region, and the resulting vector was ligated with the digested scFvHER2 gene. The ligated genes were then transformed into *E. coli* (DH5α) and selected using antibiotics (ampicillin, 50 μg/mL).

To modify gH, the scFvHER2 gene was amplified using specific primers containing a *Not*I restriction enzyme site and linker sequences (forward: 5′-CGCGGCCGCAGTAGTGGCGGTGGCTCTGGTTCCGGTGGAGAGGTGCAGCTGGTTGAAT-3′; reverse: CGCGGCCGCTCCACCGGAACCAGAGCCTCCACCGGAAGACTTGATTTCCACCTTGGTGCCC). The PCR amplification consisted as follows: 1 cycle at 95°C for 5 min, 35 cycles at 95°C for 1 min, at 60°C for 45 s, and at 72°C for 2 min, and additional extension at 72°C for 5 min. The pPEP-gH29N and scFvHER2 were digested with *Not*I, ligated, and transformed into DH5α bacteria.

### BAC engineering for modification and construction of double-retargeted oHSV-1

We generated an HVEM-restricted an oHSV-1 backbone that constructed from KOS-37 BAC plasmid[22] to evade nectin-1 binding and to increase HVEM interaction of viral gD by BAC engineering using Counter-Selection BAC Modification Kit (Gene Bridges). The modification of gD was initiated by transforming the pRed/ET

plasmid and inserting a rpsL-neo cassette armed with specific sequences by PCR. To modify the arginine and phenylalanine of gD to asparagine and isoleucine, $gD^{R222N/F223I}$ forward synthetic gene fragment was incorporated into gD by homologous recombination. To evaluate formation of virus from the BAC construct, a GFP expression cassette was incorporated between UL26 and UL27 of all BAC constructs.

The scFvEpCAM-HVEM and scFvHER2-HA expression cassettes, as well as the retargeted gH genes (gH:scFvEpCAM and gH:scFvHER2), were inserted into an HVEM-restricted HSV-1 backbone. The HVEM-restricted HSV-1 backbone was harbored in *E. coli* (DH10B) transformed with the pRed/ET plasmid. The rpsL-neo cassette was amplified by PCR with gene-specific primers tagged with arm sequences designed according to incorporation positions. The armed rpsL-neo cassette was replaced into the respective region of the HVEM-restricted HSV-1 backbone for modification by homologous recombination. The replacement of the rpsL-neo cassette was verified by antibiotics tests with chloramphenicol (15 μg/mL) and streptomycin (15 μg/mL), and colony PCR with each specific primer set. The adapter expression cassette (scFvEpCAM-HVEM and scFvHER2-HVEM) and modified gH gene (gH:scFvEpcAM and gH:scFvHER2) were amplified by PCR with their specific primers with arm sequences. The scFvEpCAM-HA was substituted with the rpsL-neo cassette by homologous recombination, and introduced between the UL3 and UL4 regions (EA-S). A gH:scFvEpcAM gene was replaced between the 29 and 30 amino acids of gH (EgH-S). The double-retargeted construct (EA-EgH-D) was generated by the insertion of gH:scFvEpCAM into EA-S. The HER2 double-retargeted construct (HA-HgH-D) was performed as described for construction of EA-EgH-D. The gene-specific primers and synthetic oligonucleotides used for BAC modification in this study were listed in Table S1. The PCR products used for BAC engineering were amplified under the following conditions: 1 cycle at 95°C for 5 min, 35 cycles of at 95°C for 1 min, at 60°C for 45 s, and at 72°C 2 min, and 1 cycle at 72°C for 5 min. All BAC-engineered constructs were verified by targeted DNA sequencing analysis and restriction enzyme digestion.

#### EpCAM-retargeted virus preparation and purification

Recombinant viruses were generated by transfecting Cre-Vero-HVEM cells using Lipofectamine 2000 (Thermo Fisher Scientific), followed by two rounds of limiting dilution on Cre-Vero-HVEM cells. The BAC region flanked by *loxP* elements was removed by Cre recombinase to avoid immunological interference by BAC-encoded elements (e.g., LacZ and chloramphenicol resistance). Propagation, purification, and titration of viruses were performed as previously described.[47] Briefly, Vero-HVEM cells were infected with the virus at an MOI of 0.01 at 37°C overnight. After total cytopathic effect was observed at 33°C, 5M NaCl, and dextran sulfate solution were added to a final concentration of 0.45 M and 100 μg/mL, respectively. The supernatant was harvested and concentrated by centrifugation at 29,000×*g* for 60 min. The virus was purified by size-exclusion chromatography using Capto core 700 beads (Cytiva). The virus titer was determined by plaque assay in Vero-HVEM cells. Vero-HVEM cells were infected with serial dilutions of the virus and incubated with DMEM supplemented with 1% FBS and 0.5% methylcellulose (Sigma) for 3–4 days until the plaques were visible. The cells were then fixed with methanol and stained with crystal violet (Sigma) for 15 min to visualize the plaques. Viral plaques were counted, and the average for each dilution was determined. The value was multiplied by 10 to the power of dilution to obtain the number of PFU per milliliter.

#### Production and purification of EpCAM adapter

EpCAM adapter was obtained through collaboration with Y-Biologics. 293F cells were transfected with appropriate expression plasmids using Lipofectamine 3000 (Thermo Fisher Scientific). The culture media were harvested and loaded onto Ni Sepharose 6 Fast Flow (Cytiva) for first purification of the His-tagged protein. The second purification was conducted using an SRT-C SEC-300 HPLC column (Sepax) on an Ultimate 3000 system (Thermo Fisher Scientific). The final purification was performed using Superdex 26/600 200 pg (Cytiv) on AKTA Go (Cytiva). Purified proteins were identified by gel electrophoresis and immunoblotting. The concentration of each purified protein was determined by Bradford assay (Bio-Rad).

#### Virus entry and spreading

Cells were seeded into a 96-well culture plate. The indicated cell lines were infected with KOSG, EgH-S, and EA-EgH-D viruses for 90 min at 37°C. For the entry of EpCAM self-targeting virus, EA-S virus was incubated with or without 125 nM EpCAM adapter for 30 min at 4°C. After the removal of unbound viruses, fresh growth media were added to each well. To assess plaque formation, infected cells were overlaid with medium containing 0.5% methylcellulose for 3 days at 37°C. Virus infection and plaques were monitored GFP fluorescence and images were collected under fluorescence microscopy, IX73 (Olympus).

#### Cell killing ability and virus replication

For the cell killing assay, cells were seeded in 96-well plates and infected with KOSG. nectin-1-detargeted KOSG, or EA-EgH-D virus at an MOI of 1 for 1–5 days. In addition, HER2-targeted HSV-1 was infected at an MOI of 2. Cell viability was determined by addition of EZ-Cytox solution (DogenBio, Korea). The $OD_{450}$ was recorded by a SpectraMax i3x ELISA reader (Molecular Devices). The curves were obtained by plotting the measured cell viability (%) against non-infected control cells using GraphPad Prism software (GraphPad). To determine virus replication, cells were seeded to 90% confluence in 12-well culture plates and infected with KOSG, nectin-1-detargeted KOSG, or EA-EgH-D virus at an MOI of 0.1. The infected cells were harvested separately at 3, 24, and 48 h after infection and subjected to five freeze-thaw cycles. Progeny virus yields were titrated in Vero-HVEM cells.

#### Animal experiments

The experimental animal procedures were approved by the Institutional Animal Care and Use Committee (IACUC) of the Korea Institute of Radiological and Medical Sciences in accordance with the

guidelines and policies of the Korean Council on Animal Care. Eight-week-old female nude mice were purchased from Charles River Laboratories and maintained under sterile conditions. All animal studies were conducted using protocols approved by the Institutional Animal Care and Use Committee of the Korea Institute of Radiological and Medical Sciences. Nude mice were s.c. injected in the right hind leg with $5 \times 10^6$ MDA-MB-453 cells. When the average size of the tumors reached about 100–150 $mm^3$, the tumor-bearing mice were randomly divided into groups. To visualize *in vivo* replication, mice with MDA-MB-453 s.c. tumors received an i.t. injection of EA-EgH-D in 20 μL volume and were killed 6, 48, and 72 h later. The resected tumors were cut in half and observed under a fluorescence *in vivo* imager. All the optical images were acquired with a Bruker *in vivo* Xtreme system (Bruker). Accurate observations of other organs did not reveal any fluorescence signal. For i.t. injection, MDA-MB-453 tumor-bearing mice received a single injection of $2 \times 10^4$, $2 \times 10^5$, and $2 \times 10^6$ PFU of EA-EgH-D or PBS. For systemic delivery, when the average tumor size reached approximately 200 $mm^3$, mice were given a single i.v. injection of $2 \times 10^6$, $2 \times 10^7$, or $2 \times 10^8$ PFU virus or PBS in the volume of 100 μL. Tumor growth was monitored by measuring tumor size with digital calipers twice a week, and tumor volumes were calculated as (length × $width^2$)/2.[48] For safety evaluation, Seven-week-old female immunocompetent FVB/N mice (DBL) were injected via tail vein with HSV-1 WT KOS strain ($1 \times 10^6$ PFU), EA-EgH-D ($1 \times 10^8$ PFU), or PBS. Infected mice were monitored daily for signs of disease, and their weight was recorded. Mice displaying severe symptoms or 20% weight loss were immediately euthanized. Survival curves were analyzed using the long-rank (Mantel-Cox) test.

### qPCR

To prepare total DNA from target organs (brain, liver, lung, and kidney), FVB/N mice were sacrificed on study day 8 and dissected to get the internal organs. The tissues were processed with DNeasy Blood & Tissue Kits (Qiagen Sciences), and total DNA from this step was stored at −20°C. HSV-1 genomic copies were measured by qRT-PCR using QuantStudio 5 Real-Time PCR System (Thermo Fisher Scientific) and analyzed by Design & Analysis 2.6. HSV type 1 (HSV-1) Real-Time PCR Assay probe/primer mix (Virusys) 50 ng total DNA extracted from a target organ was used as a template. The forward and reverse primers contain FAM/BHQ-labeled probes, which are specialized for HSV-1 gD gene. qRT-PCR was performed with one cycle of 95°C for 10 min, 45 cycles of 95°C for 10 s, and one cycle of 64°C for 1 min. The standard curve was using a virus preparation of known concentration ($10^{12}$ copies/mL) and was produced linear results at dilutions of $10^8$–$10^2$ copies per reaction. Thus, experimental values of less than $10^2$ copies were considered below the detection limit and scored as negative.

### Flow cytometry

Cells were collected and stained with PE-conjugated antibodies against EpCAM (clone #9C4; BioLegend), HER2 (clone #24D2; BioLegend), Nectin-1 (clone #R1.302; BioLegend), and HVEM (clone #94801; Norvus) for 30 min at 4°C. After washing with FACS stain buffer, cell surface markers were analyzed using flow cytometry (FACS) with a CytoFlex instrument (Beckman Coulter) and FlowJo software (FlowJo).

### Statistical analysis

Data were acquired from three independent experiments, and all error bars represent the standard error of the means. Statistical analysis was performed using GraphPad prism version 8 (GraphPad). One-way ANOVA Followed by Tukey's multiple comparison test or student's *t*-test was used to analyze the data as appropriate. Kaplan-Meier survival curves were used to present animal survival, and the log rank (Mantel-Cox) test was used to analyze survival rates. p values of less than 0.05 were considered statistically significant.

## DATA AND CODE AVAILABILITY

All data that support the findings of this study are included in this published article and Supplemental information. Raw data in this study are available from the corresponding author upon reasonable request.

## SUPPLEMENTAL INFORMATION

Supplemental information can be found online at https://doi.org/10.1016/j.omton.2024.200778.

## ACKNOWLEDGMENTS

We thank Joseph C. Glorioso and Justus B. Cohen (University of Pittsburgh School of Medicine) for offering HSV-1 wild-type KOS strain. We also thank David A. Leib (Geisel School of Medicine at Dartmouth) for providing us with the KOS-37 BAC and Cre-Vero cell lines, Aikichi Iwamoto (University of Tokyo) for the DSP assay system, and Gabriella Campadelli-Fiume (University of Bologna) for offering HSV-1-resistant cells and their derivatives. This research was supported by the Korea Drug Development Fund funded by the Ministry of Science and ICT, Ministry of Trade, Industry, and Energy, and Ministry of Health and Welfare (RS-2021-DD120799, Republic of Korea).

## AUTHOR CONTRIBUTIONS

H.B., and H.K. contributed to the design of the work. H.J. and C.A. conducted the analysis and interpretation of the data. E.P., Y.L., S.L., M.H., B.K., and Y.J. performed the experiments and analyzed the data. H.B., H.J., and H.K. wrote and edited the manuscript. H.K. supervised the study.

## DECLARATION OF INTERESTS

All authors are current or former employees of Gencellmed Inc. H.K. has intellectual property rights to the EA-EgH-D virus and is a founder of Gencellmed, Inc., which owns these rights and intends to commercialize the virus.

## REFERENCES

1. Ma, R., Li, Z., Chiocca, E.A., Caligiuri, M.A., and Yu, J. (2023). The emerging field of oncolytic virus-based cancer immunotherapy. Trends Cancer *9*, 122–139. https://doi.org/10.1016/j.trecan.2022.10.003.

2. Hemminki, O., and Hemminki, A. (2016). A century of oncolysis evolves into oncolytic immunotherapy. OncoImmunology *5*, e1074377. https://doi.org/10.1080/2162402X.2015.1074377.

3. Maroun, J., Muñoz-Alía, M., Ammayappan, A., Schulze, A., Peng, K.W., and Russell, S. (2017). Designing and building oncolytic viruses. Future Virol. *12*, 193–213. https://doi.org/10.2217/fvl-2016-0129.

4. Andtbacka, R.H.I., Kaufman, H.L., Collichio, F., Amatruda, T., Senzer, N., Chesney, J., Delman, K.A., Spitler, L.E., Puzanov, I., Agarwala, S.S., et al. (2015). Talimogene Laherparepvec Improves Durable Response Rate in Patients With Advanced Melanoma. J. Clin. Oncol. *33*, 2780–2788. https://doi.org/10.1200/JCO.2014.58.3377.

5. Rehman, H., Silk, A.W., Kane, M.P., and Kaufman, H.L. (2016). Into the clinic: Talimogene laherparepvec (T-VEC), a first-in-class intratumoral oncolytic viral therapy. J. Immunother. Cancer *4*, 53. https://doi.org/10.1186/s40425-016-0158-5.

6. Frampton, J.E. (2022). Teserpaturev/G47Delta: First Approval. BioDrugs *36*, 667–672. https://doi.org/10.1007/s40259-022-00553-7.

7. Coffin, R.S. (2015). From virotherapy to oncolytic immunotherapy: where are we now? Curr. Opin. Virol. *13*, 93–100. https://doi.org/10.1016/j.coviro.2015.06.005.

8. Gatta, V., Petrovic, B., and Campadelli-Fiume, G. (2015). The Engineering of a Novel Ligand in gH Confers to HSV an Expanded Tropism Independent of gD Activation by Its Receptors. PLoS Pathog. *11*, e1004907. https://doi.org/10.1371/journal.ppat.1004907.

9. Zhou, G., Ye, G.J., Debinski, W., and Roizman, B. (2002). Engineered herpes simplex virus 1 is dependent on IL13Ralpha 2 receptor for cell entry and independent of glycoprotein D receptor interaction. Proc. Natl. Acad. Sci. USA *99*, 15124–15129. https://doi.org/10.1073/pnas.232588699.

10. Kamiyama, H., Zhou, G., and Roizman, B. (2006). Herpes simplex virus 1 recombinant virions exhibiting the amino terminal fragment of urokinase-type plasminogen activator can enter cells via the cognate receptor. Gene Ther. *13*, 621–629. https://doi.org/10.1038/sj.gt.3302685.

11. Grandi, P., Fernandez, J., Szentirmai, O., Carter, R., Gianni, D., Sena-Esteves, M., and Breakefield, X.O. (2010). Targeting HSV-1 virions for specific binding to epidermal growth factor receptor-vIII-bearing tumor cells. Cancer Gene Ther. *17*, 655–663. https://doi.org/10.1038/cgt.2010.22.

12. Uchida, H., Marzulli, M., Nakano, K., Goins, W.F., Chan, J., Hong, C.S., Mazzacurati, L., Yoo, J.Y., Haseley, A., Nakashima, H., et al. (2013). Effective treatment of an orthotopic xenograft model of human glioblastoma using an EGFR-retargeted oncolytic herpes simplex virus. Mol. Ther. *21*, 561–569. https://doi.org/10.1038/mt.2012.211.

13. Baek, H., Uchida, H., Jun, K., Kim, J.H., Kuroki, M., Cohen, J.B., Glorioso, J.C., and Kwon, H. (2011). Bispecific adapter-mediated retargeting of a receptor-restricted HSV-1 vector to CEA-bearing tumor cells. Mol. Ther. *19*, 507–514. https://doi.org/10.1038/mt.2010.207.

14. Nakano, K., Asano, R., Tsumoto, K., Kwon, H., Goins, W.F., Kumagai, I., Cohen, J.B., and Glorioso, J.C. (2005). Herpes simplex virus targeting to the EGF receptor by a gD-specific soluble bridging molecule. Mol. Ther. *11*, 617–626. https://doi.org/10.1016/j.ymthe.2004.12.012.

15. Uchida, H., Shah, W.A., Ozuer, A., Frampton, A.R., Jr., Goins, W.F., Grandi, P., Cohen, J.B., and Glorioso, J.C. (2009). Generation of herpesvirus entry mediator (HVEM)-restricted herpes simplex virus type 1 mutant viruses: resistance of HVEM-expressing cells and identification of mutations that rescue nectin-1 recognition. J. Virol. *83*, 2951–2961. https://doi.org/10.1128/JVI.01449-08.

16. Hemminki, A., Wang, M., Hakkarainen, T., Desmond, R.A., Wahlfors, J., and Curiel, D.T. (2003). Production of an EGFR targeting molecule from a conditionally replicating adenovirus impairs its oncolytic potential. Cancer Gene Ther. *10*, 583–588. https://doi.org/10.1038/sj.cgt.7700606.

17. Carette, J.E., Graat, H.C.A., Schagen, F.H.E., Mastenbroek, D.C.J., Rots, M.G., Haisma, H.J., Groothuis, G.M.M., Schaap, G.R., Bras, J., Kaspers, G.J.L., et al. (2007). A conditionally replicating adenovirus with strict selectivity in killing cells expressing epidermal growth factor receptor. Virology *361*, 56–67. https://doi.org/10.1016/j.virol.2006.11.011.

18. Verheije, M.H., Lamfers, M.L.M., Würdinger, T., Grinwis, G.C.M., Gerritsen, W.R., van Beusechem, V.W., and Rottier, P.J.M. (2009). Coronavirus genetically redirected to the epidermal growth factor receptor exhibits effective antitumor activity against a malignant glioblastoma. J. Virol. *83*, 7507–7516. https://doi.org/10.1128/JVI.00495-09.

19. van Beusechem, V.W., Mastenbroek, D.C.J., van den Doel, P.B., Lamfers, M.L.M., Grill, J., Würdinger, T., Haisma, H.J., Pinedo, H.M., and Gerritsen, W.R. (2003). Conditionally replicative adenovirus expressing a targeting adapter molecule exhibits enhanced oncolytic potency on CAR-deficient tumors. Gene Ther. *10*, 1982–1991. https://doi.org/10.1038/sj.gt.3302103.

20. Verheije, M.H., and Rottier, P.J.M. (2012). Retargeting of viruses to generate oncolytic agents. Adv. Virol. *2012*, 798526. https://doi.org/10.1155/2012/798526.

21. Gires, O., Pan, M., Schinke, H., Canis, M., and Baeuerle, P.A. (2020). Expression and function of epithelial cell adhesion molecule EpCAM: where are we after 40 years? Cancer Metastasis Rev. *39*, 969–987. https://doi.org/10.1007/s10555-020-09898-3.

22. Gierasch, W.W., Zimmerman, D.L., Ward, S.L., Vanheyningen, T.K., Romine, J.D., and Leib, D.A. (2006). Construction and characterization of bacterial artificial chromosomes containing HSV-1 strains 17 and KOS. J. Virol. Methods *135*, 197–206. https://doi.org/10.1016/j.jviromet.2006.03.014.

23. Douglas, J.T., Rogers, B.E., Rosenfeld, M.E., Michael, S.I., Feng, M., and Curiel, D.T. (1996). Targeted gene delivery by tropism-modified adenoviral vectors. Nat. Biotechnol. *14*, 1574–1578. https://doi.org/10.1038/nbt1196-1574.

24. Würdinger, T., Verheije, M.H., Broen, K., Bosch, B.J., Haijema, B.J., de Haan, C.A.M., van Beusechem, V.W., Gerritsen, W.R., and Rottier, P.J.M. (2005). Soluble receptor-mediated targeting of mouse hepatitis coronavirus to the human epidermal growth factor receptor. J. Virol. *79*, 15314–15322. https://doi.org/10.1128/JVI.79.24.15314-15322.2005.

25. Kashentseva, E.A., Seki, T., Curiel, D.T., and Dmitriev, I.P. (2002). Adenovirus targeting to c-erbB-2 oncoprotein by single-chain antibody fused to trimeric form of adenovirus receptor ectodomain. Cancer Res. *62*, 609–616.

26. Kloos, A., Woller, N., Gürlevik, E., Ureche, C.I., Niemann, J., Armbrecht, N., Martin, N.T., Geffers, R., Manns, M.P., Gerardy-Schahn, R., and Kühnel, F. (2015). PolySia-Specific Retargeting of Oncolytic Viruses Triggers Tumor-Specific Immune Responses and Facilitates Therapy of Disseminated Lung Cancer. Cancer Immunol. Res. *3*, 751–763. https://doi.org/10.1158/2326-6066.CIR-14-0124-T.

27. Dmitriev, I., Kashentseva, E., Rogers, B.E., Krasnykh, V., and Curiel, D.T. (2000). Ectodomain of coxsackievirus and adenovirus receptor genetically fused to epidermal growth factor mediates adenovirus targeting to epidermal growth factor receptor-positive cells. J. Virol. *74*, 6875–6884. https://doi.org/10.1128/jvi.74.15.6875-6884.2000.

28. Hemminki, A., Dmitriev, I., Liu, B., Desmond, R.A., Alemany, R., and Curiel, D.T. (2001). Targeting oncolytic adenoviral agents to the epidermal growth factor pathway with a secretory fusion molecule. Cancer Res. *61*, 6377–6381.

29. de Gruijl, T.D., and van de Ven, R. (2012). Chapter six–Adenovirus-based immunotherapy of cancer: promises to keep. Adv. Cancer Res. *115*, 147–220. https://doi.org/10.1016/B978-0-12-398342-8.00006-9.

30. Kwon, H., Bai, Q., Baek, H.J., Felmet, K., Burton, E.A., Goins, W.F., Cohen, J.B., and Glorioso, J.C. (2006). Soluble V domain of Nectin-1/HveC enables entry of herpes simplex virus type 1 (HSV-1) into HSV-resistant cells by binding to viral glycoprotein D. J. Virol. *80*, 138–148. https://doi.org/10.1128/JVI.80.1.138-148.2006.

31. Baek, H., Kim, J.H., Noh, Y.T., and Kwon, H. (2012). The soluble amino-terminal region of HVEM mediates efficient herpes simplex virus type 1 infection of gD receptor-negative cells. Virol. J. *9*, 15. https://doi.org/10.1186/1743-422X-9-15.

32. Uchida, H., Hamada, H., Nakano, K., Kwon, H., Tahara, H., Cohen, J.B., and Glorioso, J.C. (2018). Oncolytic Herpes Simplex Virus Vectors Fully Retargeted to Tumor- Associated Antigens. Curr. Cancer Drug Targets *18*, 162–170. https://doi.org/10.2174/1568009617666170206105855.

33. Goins, W.F., Hall, B., Cohen, J.B., and Glorioso, J.C. (2016). Retargeting of herpes simplex virus (HSV) vectors. Curr. Opin. Virol. *21*, 93–101. https://doi.org/10.1016/j.coviro.2016.08.007.

34. Leoni, V., Gatta, V., Casiraghi, C., Nicosia, A., Petrovic, B., and Campadelli-Fiume, G. (2017). A Strategy for Cultivation of Retargeted Oncolytic Herpes Simplex Viruses in Non-cancer Cells. J. Virol. *91*, e00067-17. https://doi.org/10.1128/JVI.00067-17.

35. Macedo, N., Miller, D.M., Haq, R., and Kaufman, H.L. (2020). Clinical landscape of oncolytic virus research in 2020. J. Immunother. Cancer *8*, e001486. https://doi.org/10.1136/jitc-2020-001486.

36. Shui, J.W., and Kronenberg, M. (2013). HVEM: An unusual TNF receptor family member important for mucosal innate immune responses to microbes. Gut Microb. *4*, 146–151. https://doi.org/10.4161/gmic.23443.

37. Kopp, S.J., Ranaivo, H.R., Wilcox, D.R., Karaba, A.H., Wainwright, M.S., and Muller, W.J. (2014). Herpes simplex virus serotype and entry receptor availability alter CNS disease in a mouse model of neonatal HSV. Pediatr. Res. *76*, 528–534. https://doi.org/10.1038/pr.2014.135.

38. Currier, M.A., Gillespie, R.A., Sawtell, N.M., Mahller, Y.Y., Stroup, G., Collins, M.H., Kambara, H., Chiocca, E.A., and Cripe, T.P. (2008). Efficacy and safety of the oncolytic herpes simplex virus rRp450 alone and combined with cyclophosphamide. Mol. Ther. *16*, 879–885. https://doi.org/10.1038/mt.2008.49.

39. Brudno, J.N., and Kochenderfer, J.N. (2016). Toxicities of chimeric antigen receptor T cells: recognition and management. Blood *127*, 3321–3330. https://doi.org/10.1182/blood-2016-04-703751.

40. Sasso, E., Froechlich, G., Cotugno, G., D'Alise, A.M., Gentile, C., Bignone, V., De Lucia, M., Petrovic, B., Campadelli-Fiume, G., Scarselli, E., et al. (2020). Replicative conditioning of Herpes simplex type 1 virus by Survivin promoter, combined to ERBB2 retargeting, improves tumour cell-restricted oncolysis. Sci. Rep. *10*, 4307. https://doi.org/10.1038/s41598-020-61275-w.

41. Perng, G.C., Dunkel, E.C., Geary, P.A., Slanina, S.M., Ghiasi, H., Kaiwar, R., Nesburn, A.B., and Wechsler, S.L. (1994). The latency-associated transcript gene of herpes simplex virus type 1 (HSV-1) is required for efficient in vivo spontaneous reactivation of HSV-1 from latency. J. Virol. *68*, 8045–8055. https://doi.org/10.1128/JVI.68.12.8045-8055.1944.

42. Koshizuka, T., Goshima, F., Takakuwa, H., Nozawa, N., Daikoku, T., Koiwai, O., and Nishiyama, Y. (2002). Identification and characterization of the UL56 gene product of herpes simplex virus type 2. Virol *76*, 6718–6728. https://doi.org/10.1128/jvi.76.13.6718-6728.2002.

43. Farrera-Sal, M., Moreno, R., Mato-Berciano, A., Maliandi, M.V., Bazan-Peregrino, M., and Alemany, R. (2021). Hyaluronidase expression within tumors increases virotherapy efficacy and T cell accumulation. Mol. Ther. Oncolytics *22*, 27–35. https://doi.org/10.1016/j.omto.2021.05.009.

44. Kailayangiri, S., Altvater, B., Wiebel, M., Jamitzky, S., and Rossig, C. (2020). Overcoming Heterogeneity of Antigen Expression for Effective CAR T Cell Targeting of Cancers. Cancers *12*, 1075. https://doi.org/10.3390/cancers12051075.

45. Levine, M., Goldin, A.L., and Glorioso, J.C. (1980). Persistence of herpes simplex virus genes in cells of neuronal origin. J. Virol. *35*, 203–210. https://doi.org/10.1128/JVI.35.1.203-210.1980.

46. Pertel, P.E., Fridberg, A., Parish, M.L., and Spear, P.G. (2001). Cell fusion induced by herpes simplex virus glycoproteins gB, gD, and gH-gL requires a gD receptor but not necessarily heparan sulfate. Virology *279*, 313–324. https://doi.org/10.1006/viro.2000.0713.

47. Marconi, P., and Manservigi, R. (2014). Herpes simplex virus growth, preparation, and assay. Methods Mol. Biol. *1144*, 19–29. https://doi.org/10.1007/978-1-4939-0428-0_2.

48. Tomayko, M.M., and Reynolds, C.P. (1989). Determination of subcutaneous tumor size in athymic (nude) mice. Cancer Chemother. Pharmacol. *24*, 148–154. https://doi.org/10.1007/BF00300234.